Comparison and evaluation of spatial interpolation schemes for daily rainfall in data scarce regions

Paul D. Wagner [a], Peter Fiener [a,b], Florian Wilken [a], Shamita Kumar [c], Karl Schneider [a,*]

[a] Hydrogeography and Climatology Research Group, Institute of Geography, University of Cologne, D-50923 Köln, Germany
[b] Indo-German Centre of Sustainability, Indian Institute of Technology Madras, Chennai 600 036, India
[c] Institute of Environment Education & Research, Bharati Vidyapeeth University, Pune 411 043, India

Keywords:
Rainfall
Interpolation
Kriging
SWAT
TRMM
India

S U M M A R Y

Accurate rainfall data are of prime importance for many environmental applications. To provide spatially distributed rainfall data, point measurements are interpolated. However, in low density measurement networks, the use of different interpolation methods may result in large differences and hence in deviations from the actual spatial distribution of rainfall. Our study aims at analyzing different rainfall interpolation schemes with regard to their suitability to produce spatial rainfall estimates in a monsoon dominated region with scarce rainfall measurements. The study was carried out in the meso-scale catchment of the Mula and the Mutha Rivers (2036 km^2) upstream of the city of Pune, India. Rainfall data from 16 rain gauges were spatially interpolated using seven different methods, including Thiessen polygons, statistical, and geostatistical approaches. The two most suitable covariates for rainfall interpolation were identified as (i) distance in wind direction from the main orographic barrier and as (ii) a 0.05° pattern of mean annual rainfall derived from satellite data acquired by the Tropical Rainfall Measuring Mission (TRMM). Consequently, these two covariates were used in the regression-based interpolation approaches. The quality of the different methods was assessed using a two step validation approach: (i) Cross-validation was used to evaluate the capability to reproduce measured data. (ii) Spatially integrated interpolation performance was assessed by using a hydrologic model to calculate runoff and compare modeled to measured runoff. By this assessment, the regression-based methods showed the best performance. We found that the choice of the covariate had a significant impact on precipitation and runoff amounts, as well as on the temporal course of runoff events. Our results show, that the decision on the suitable interpolation scheme should not only be based on the comparison with point measurements, but should also take the representativeness of the given measurement network as well as of the interpolated spatial rainfall distribution into account. The successful application of regression-based interpolation methods using a high resolution TRMM pattern as covariate is very promising as it is transferable to other data scarce regions.

1. Introduction

Accurate precipitation data are of prime importance for many environmental studies, especially if related to water resources. At small scales, the use of measurements from individual rain gauges might be appropriate. However at larger scales, it is required to draw special attention to the appropriate representation of the spatial precipitation patterns, which are usually interpolated from point measurements (Chaubey et al., 1999; Tabios and Salas, 1985; Zhang and Srinivasan, 2009). A wide range of interpolation methods is available, ranging from simple techniques such as Thiessen polygons (Thiessen, 1911) or inverse distance weighting schemes (Di Piazza et al., 2011; Teegavarapu et al., 2009) to more complex and computationally intensive approaches such as geostatistical kriging (Buytaert et al., 2006; Zhang and Srinivasan, 2009). The more complex approaches often use additional information from static (e.g., elevation) or dynamic (e.g., rainfall radar) covariates that are available as spatially distributed data sets.

In many regions of the world, precipitation measurements are scarce and interpolation is not only more important, but also more difficult (Croke et al., 2011). Since spatial patterns are often more heterogeneous and pronounced at short time scales, an appropriate interpolation scheme is particularly important at short time scales such as daily or hourly precipitation. These short time steps are usually required for distributed hydrologic modeling studies, and model accuracy critically depends on these input data (Beven, 2001). Nevertheless in data scarce regions, the use of simple

* Corresponding author. Tel.: +49 221 470 4331; fax: +49 221 470 5124.
E-mail address: karl.schneider@uni-koeln.de (K. Schneider).

approaches is very common (e.g., Croke et al., 2011; Ndomba et al., 2008; Stehr et al., 2008). Especially with regard to daily values, the application of more complex interpolation schemes is relatively rare (e.g., Buytaert et al., 2006), although these may lead to substantial improvements in hydrologic model performance (Stehr et al., 2008). In general, complex methods are more commonly used, when data availability is sufficient (Hattermann et al., 2005; Ly et al., 2011; Zhang and Srinivasan, 2009) or with coarser time resolution (e.g., annual data, Basistha et al., 2008).

In case of coarse measurement networks, interpolation schemes that include additional information from covariates are most promising as they may (partly) compensate for the low network density. Particularly for precipitation, covariates can substantially improve the representation of spatial patterns (Verworn and Haberlandt, 2011). Suitable and applicable covariates should be available at a higher spatial resolution and be inexpensive to measure in comparison to the interpolated variable (Burrough and McDonnell, 1998). A further requisite of a covariate is that it should – to some extent – explain the interpolated variable. This characteristic is typically given by a process that links the covariate to the variable and is proven by a regression analysis based on the available data. Traditionally, elevation or other parameters extracted from digital elevation models (DEMs) are used for rainfall interpolation (Buytaert et al., 2006; Goovaerts, 2000; Kurtzman et al., 2009; Lloyd, 2005; Verworn and Haberlandt, 2011). Satellite products, especially from radar remote sensing, are increasingly used as covariates, since they provide spatially detailed information of rainfall distribution (Velasco-Forero et al., 2009; Verworn and Haberlandt, 2011; Schiemann et al., 2011). Furthermore, interpolation methods that use remotely sensed observations can easily be transferred to different regions, whereas other covariates (e.g., elevation; Lloyd, 2005) are often suitable only for a specific region or time of the year, depending on local climatic conditions. The spatially detailed information provided by satellite data is even more valuable in the context of data scarce regions.

Another difficulty associated with applying interpolation schemes in data scarce regions is the accuracy assessment. Usually interpolation results are evaluated applying cross-validation techniques (Hattermann et al., 2005; Lloyd, 2005). Unfortunately, the accuracy of this validation method depends on the number and the location of the gauges within the study area, which should be representative of the distribution of rainfall in space. These criteria are hardly met in case of a limited number of measurements, as rain gauges are often found close to settlements to reduce maintenance efforts. Additional more robust validation is often difficult to achieve and is mostly of a qualitative nature, e.g., comparison and analysis of interpolated rainfall patterns (Carrera-Hernández and Gaskin, 2007; Lloyd, 2005; Velasco-Forero et al., 2009). However, a qualitative, manual assessment of interpolation techniques is not feasible, if interpolation is carried out for a time series (e.g., on a daily time step). Furthermore, spatially integrated assessment of interpolation accuracy would be highly favorable. Zhang and Srinivasan (2009) include areal mean precipitation amounts into the comparison of different interpolation methods. This approach can be enhanced by the application of a hydrologic model. Such a modeling approach not only provides temporally and spatially integrating information in the sense of a water balance study, it also provides a spatially integrating and temporally explicit perspective through the analysis of the modeled hydrograph. Thus, results of different precipitation interpolation schemes may be used as inputs to hydrologic models to analyze their effect upon modeled runoff. The approach of using a hydrologic model to assess the performance of different interpolation schemes has previously been used in several studies (e.g. Cole and Moore, 2008; Gourley and Vieux, 2005; Heistermann and Kneis, 2011; Hwang et al., 2012). This method is especially relevant in catchments that are dominated by heavy rainfall events, producing mostly direct runoff and resulting in highly dynamic hydrographs, which allow for a simple evaluation of the rainfall inputs.

Particularly in mountainous areas, spatial patterns are consistently affected by topography and wind direction (Barros and Lettenmaier, 1993; Barry, 1992). This is the case in the Western Ghats, India, where topography and monsoon winds result in spatially highly variable rainfall, which is largely determined by orographic lift and foehn effects. In a previous study carried out in the meso-scale catchment of the Mula and the Mutha Rivers upstream of the city of Pune, India, precipitation input was identified as a major source of error for runoff modeling (Wagner et al., 2011).

The main objective of this paper is to analyze different rainfall interpolation schemes with regard to their suitability to produce spatial rainfall estimates on a daily time step in a monsoon dominated region with scarce precipitation measurements. A special focus is set on the identification of an appropriate and transferable covariate and on the validation of the interpolation schemes using hydrologic modeling results and measured runoff.

2. Materials and methods

2.1. Study area

The meso-scale catchment of the Mula and the Mutha Rivers (2036 km^2) is located in the Western Ghats upstream of the city of Pune (18.53°N, 73.85°E; Fig. 1). It is a sub-basin and source area of the Krishna River, which drains towards the east and into the Bay of Bengal. Its elevation ranges from 550 m in Pune up to 1300 m.a.s.l. on the top ridges in the Western Ghats. The catchment has a tropical wet and dry climate, which is characterized

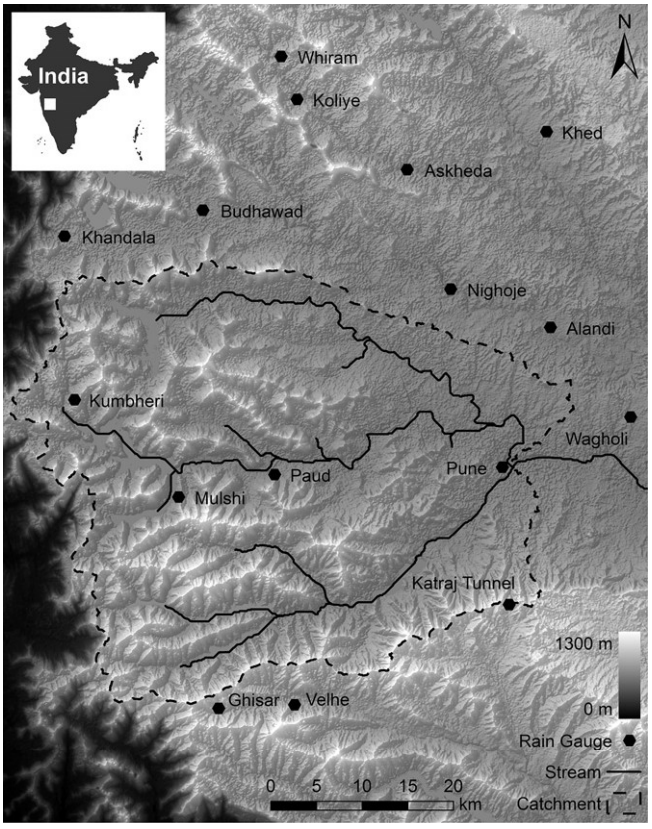

Fig. 1. Topography of the study area with the Mula–Mutha catchment and the available rain gauges.

by seasonal rainfall from June to October and low annual temperature variations with an annual mean of 25 °C at the catchment outlet in Pune. Annual rainfall amounts decrease from approximately 3500 mm in the western to 750 mm in the eastern part of the catchment (Gadgil, 2002; Gunnell, 1997). Land use is dominated by semi-natural vegetation, with forests (20.6%) mainly on the higher elevations in the west, whereas shrubland (26.6%) and grassland (22.8%) occupy lower elevations. Agriculture comprises only 10.6% of the catchment and is mainly located in proximity to rivers and to six large dams (5.8% of the catchment is covered by water). Agriculture is dominated by small fields (<1 ha) with rain-fed agriculture during the monsoon season and irrigation during the dry season. Typically two crops per year are harvested. Urban area (13%) is mainly found in the eastern part of the catchment, where the city of Pune and its surrounding settlements are situated (Wagner et al., 2011).

2.2. Precipitation data

Daily measurements of precipitation at 16 gauges within or close to the catchment (Fig. 1) were provided by the Water Resources Department Nashik and the Indian Meteorological Department (IMD) Pune. Measurements are carried out with a Symon's rain gauge, which is the Indian standard gauge (Jain et al., 2007). It measures rainfall at a height of 30 cm above ground level. The surface area of the gauge is 200 cm^2. The gauge is typically installed on a concrete foundation block (60 × 60 × 60 cm) embedded in the ground. A fence (5.5 × 5.5 m) secures a minimum distance to possibly measurement interfering objects like bushes. Furthermore, such gauges should not be unduly exposed to wind (Jain et al., 2007). Twenty-four hour rainfall sums are given for each day at 8:30 a.m. Indian Standard Time. Ten of these gauges are operated manually, whereas six are self-recording gauges. Five of the latter only recorded data during the monsoon season. To provide accurate daily precipitation data, the following processing steps were applied: (i) quality control, (ii) filling of data gaps, (iii) correction of systematic measurement errors, and (iv) analysis of three different interpolation schemes.

2.2.1. Quality control, gap filling, and error correction

Daily precipitation measurements were available to this study from all 16 rain gauges. The data was tested for consistency using double mass curves (Searcy et al., 1960). Due to the higher amounts of rainfall and larger number of rain days in the upper catchment, gauges within the western part and gauges within the eastern part were tested separately. The 73.7°E longitude was used to divide the data set into gauges recording more (west) or less (east) than 1500 mm mean annual rainfall. For both parts of the catchment, one reliable rain gauge with a continuous data set was chosen as reference. The gauge in Pune, which is maintained by the IMD, is possibly one of the most reliable gauges in the catchment, because its record covers the entire period from 1988 to 2008 and had only one missing value. Due to its central location in the east, it was chosen as the reference gauge for the eastern part of the catchment. For the western part, the central gauge in Paud was used, as its record shows no missing value from 1988 to 2008. The cumulative sums of each of the other stations were compared to their respective reference station on a daily basis. If the double mass curves showed inconsistencies (e.g., steps or a change in slope), the data were checked and questionable data were marked as missing values (e.g., in some cases missing values are given as 0 mm in the original data sheet). Apart from questionable values some shifts in time were detected. Since inconsistent double mass curves on a daily time step could also result from other effects such as local thunderstorms, data were only corrected, if there was clear evidence from other gauges (e.g., a time shift was only corrected, if comparisons with all neighboring gauges indicated the shift).

Thereafter, the missing values were filled using a regression-based gap filling approach. The available data at the gauge with data gaps was summed up for each year. Corresponding annual precipitation sums were calculated for every gauge using the same dates. On this basis, a linear regression was carried out to establish a relationship between the station with the incomplete data and each of the other stations. The slope of the regression was used as a factor to estimate missing data at the incomplete station from each of the other gauges. To identify the most suitable gauge to fill the incomplete station, 120 randomly chosen precipitation days (4 months) were estimated from each of the other rain gauges. Subsequently the root mean square error (RMSE) was calculated to evaluate the performance of each gauge. This procedure was repeated 10 times, providing a mean RMSE to identify the most suitable gauge. Filling was not applied, if measurements for a whole year were missing. Thus, the derived precipitation data set consists of 10 gauges with complete daily records from 1988 to 2008 and six gauges with gaps that comprised one or more years.

Finally, to account for the systematic undercatch of precipitation measurements due to wind loss, wetting loss, and evaporation a correction method developed by Richter (1995) was applied. This method that had been developed for the German measurement network was chosen, since a specific method for India was not available. It estimates precipitation errors based on precipitation type and wind exposition (shielding) of the rain gauge. To account for the precipitation character and rain gauge setup in the catchment, we chose the coefficients for German summer rain and light shielding (Richter, 1995). Depending on the rain gauge location, the correction adds between 2.9% (106 mm mean annual rainfall) and 7.4% (40 mm mean annual rainfall) to the measured rainfall amounts.

2.3. Interpolation schemes

Seven different interpolation schemes (Table 1) that use data from the Mula–Mutha catchment and its surroundings (Fig. 1) were applied and compared. These interpolation schemes were carried out on a 1 km^2 grid. Inputs for the hydrologic model were derived from this grid by averaging the gridded rainfall values for each sub-basin used in the model. Two sets of interpolation schemes were tested: (i) univariate methods and (ii) regression-based methods, which incorporate additional information from covariates.

2.3.1. Univariate interpolation methods

As a reference, Thiessen polygons (Thiessen, 1911) were used. Each grid point was assigned the value of the nearest rain gauge. This simple approach balances the contributions of the nearest gauges within each sub-basin and is therefore superior to simply using

Table 1
Spatial interpolation schemes for daily rainfall interpolation.

Method	Interpolation scheme	Covariate	Abbreviation
1	Thiessen polygons	–	TH
2	Inverse distance weighting	–	IDW
3	Ordinary kriging	–	OK
4a	Regression–inverse distance weighting	(a) *X*-coordinate	$RIDW_X$
4b		(b) TRMM pattern	$RIDW_{TRMM}$
5a	Regression–kriging	(a) *X*-coordinate	RK_X
5b		(b) TRMM pattern	RK_{TRMM}

the nearest rain gauge, which is the standard method implemented in the ArcSWAT model setup interface (Winchell et al., 2010).

Inverse distance weighting (IDW) is a widely used and easy to implement interpolation method. The influence of the measured point data $z(x_i)$ is weighted according to the distance d_{0i} from the sampled point x_i to the estimated point x_0. Based on the optimal cross-validation performance the exponent of one was chosen, providing better estimates in this study than the frequently used standard exponent of two (Heistermann and Kneis, 2011; Shepard, 1968). The weights λ_i can hence be calculated as

$$\lambda_i = \frac{d_{0i}^{-1}}{\sum_{j=1}^{n} d_{0j}^{-1}}. \quad (1)$$

In our case we used a localized IDW approach that only takes the values of the n gauges within a 30 km distance into account. Thus the value at the interpolated location is estimated as

$$\hat{z}(x_0) = \sum_{i=1}^{n} \lambda_i \cdot z(x_i), \quad \text{where} \quad \sum_{i=1}^{n} \lambda_i = 1. \quad (2)$$

Thirdly, an ordinary kriging scheme (OK) was evaluated. Analogous to the IDW scheme, weights are calculated for every sampled point, but in contrast to IDW, the weights $\lambda_O(i)$ are optimized based on the information that is inherent in the measured data. The weights are obtained by solving the system

$$\sum_{i=1}^{n} \lambda_O(i)\gamma(x_i, x_j) + \phi = \gamma(x_j, x_0) \text{ for all } j$$
$$\sum_{i=1}^{n} \lambda_O(i) = 1, \quad (3)$$

where $\gamma(x_i, x_j)$ represents the value of the semivariogram function for the distance between the points x_i and x_j, $\gamma(x_j, x_0)$ is the value for the distance between x_j and the estimated location x_0, and ϕ is the Lagrange parameter. The semivariogram function is derived by fitting a semivariogram model to the empirical semivariogram, which can be calculated for all distances h by solving

$$\hat{\gamma}(h) = \frac{1}{2n} \sum_{i=1}^{n} (z(x_i) - z(x_i + h))^2. \quad (4)$$

Point estimates are calculated by using the optimized weights $\lambda_O(i)$ instead of the IDW weights λ_i in formula (2). Further theoretical details on geostatistics are available in the literature (e.g., Wackernagel, 2003; Webster and Oliver, 2007).

Geostatistical methods are commonly used for spatial interpolation of rainfall (Goovaerts, 2000; Zhang and Srinivasan, 2009). However, to detect spatial autocorrelation, at least 100 measurement locations (ideally 150) are required to supply a sufficient number of data pairs, which is evidently needed to derive an accurate empirical semivariogram (Webster and Oliver, 2007). Furthermore, variogram analysis and fitting of variogram models is very important and should be carried out manually, as it requires considerable judgment and skill (Burrough and McDonnell, 1998). To meet these requirements, pooled semivariograms (Fiener and Auerswald, 2009; Schuurmans et al., 2007; Voltz and Webster, 1990) for each month were used. These pooled semivariograms were calculated from mean daily precipitation values for every month in every year. The monthly values of the individual years were treated as spatially independent measurements, resulting in 312 data sets per month (21 years $*$ 16 stations – 24 years missing at different stations) that give 1938 point pairs for every semivariogram, which were grouped into 14 lag classes. A Matern semivariogram model was fitted to these empirical semivariograms (Fig. 2). This model is recommended for interpolation of spatial data (Stein, 1999) and includes as special case the Gaussian model, which Ly et al. (2011) recommend for rainfall interpolation. On this basis,

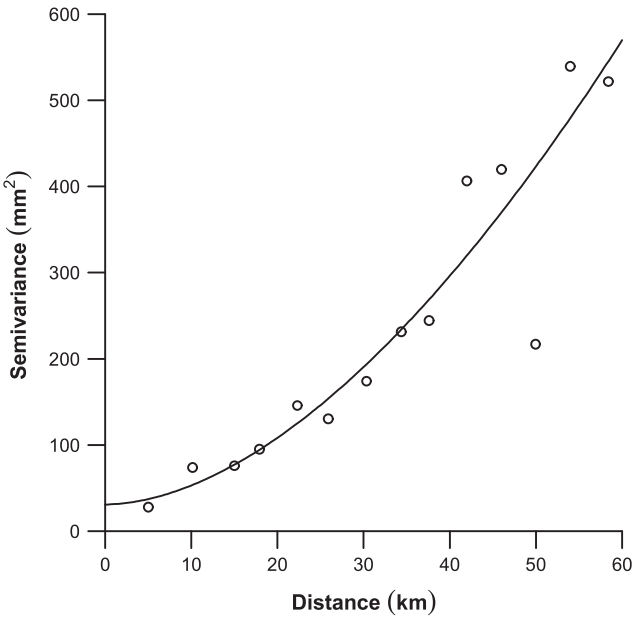

Fig. 2. Semivariogram and fitted Matern model for pooled July rainfall data (1988–2008).

a local kriging approach was applied taking only stations within a 30 km distance into account. Due to the small number of rain days in dry season months, variograms of mean monthly rainfall are not useful for interpolation of the rare rainfall events in this period. Therefore, kriging was only applied from June to September, whereas IDW was used in the remaining months. All interpolations and geostatistical analyses were carried out using the statistical software GNU R, version 2.13.0 (R Development Core Team, 2011) and the add-on package gstat (Pebesma, 2004).

2.3.2. Covariates for rainfall interpolation

The use of covariates can substantially improve interpolation results. In principal, a spatially distributed variable is utilized to estimate rainfall amounts. To identify appropriate, easily available and spatially distributed covariates, a linear regression between mean annual rainfall and the value of the covariates at the rain gauges was carried out. Four covariates were taken into account: (i) elevation, (ii) distance from the main orographic barrier in main wind direction, (iii) *X*-coordinate, (iv) a pattern of mean annual rainfall derived from satellite data acquired by the Tropical Rainfall Measuring Mission (TRMM).

Elevation is commonly used as a covariate for precipitation (e.g., Buytaert et al., 2006; Goovaerts, 2000; Kurtzman et al., 2009; Lloyd, 2005; Verworn and Haberlandt, 2011), but in our case there was no significant correlation between rainfall and elevation data (Table 2). The distance in the main south-west (SW) wind direction from the main orographic barrier in the region, the Western Ghats escarpment, provides a high coefficient of determination. The escarpment marks the sharp decline from the Western Ghats

Table 2
Capability of different covariates to represent mean annual rainfall data, as indicated by the coefficient of determination (R^2) and the *p*-value.

Covariate	R^2	Significance
Elevation	0.07	$p = 0.32$
Distance from the Western Ghats escarpment in main wind direction (SW)	0.84	$p < 0.001$
X-coordinate	0.92	$p < 0.001$
TRMM pattern	0.83	$p < 0.001$

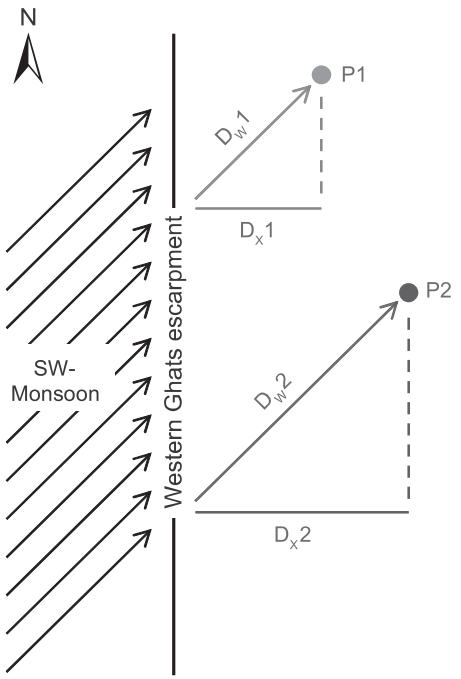

Fig. 3. Proportionality of the distance in main wind direction (D_W) and the distance in east–west direction (D_X) from the Western Ghats escarpment for any location P in the catchment.

mountain range to the coastal plain, which also constitutes the western boundary of the catchment (Fig. 1). Due to the general north–south direction of the Western Ghats escarpment, the distance from the escarpment (in east–west direction) is proportional to the distance in wind direction from the escarpment (Fig. 3) for any location in the catchment and all western wind directions. Thus, this east–west-distance, which can be expressed by the UTM *X*-coordinate, represents the downwind fetch and consequently, the west to east decline of precipitation starting from the escarpment. Since the *X*-coordinate is valid for all western wind directions, it is superior to the distance from the escarpment in SW wind direction. This becomes obvious in the higher coefficient of determination (Table 2). An additional advantage of this covariate is its simplicity of calculation. However, spatial transferability of this covariate to different regions is obviously limited.

A pattern of mean annual rainfall was derived from the Precipitation Radar (PR) instrument of the Tropical Rainfall Measuring Mission (TRMM). The TRMM product 2A25 provides a near-surface rainfall rate estimated from the precipitation radar at a 4.3 km resolution. All available observations between 1998 and 2008 were used and remapped to 0.05° resolution by the Earth System Science Interdisciplinary Center, University of Maryland and NASA/Goddard Space Flight Center. The PR system is stable and accurate enough to allow for quantitative radar reflectivity (Kummerow et al., 2000). Due to the orbital period of the TRMM satellite, the number of observations has an effect on uncertainty of the derived annual rainfall pattern. However, Kidd and McGregor (2007) demonstrated the use of seasonal rainfall patterns acquired from a shorter period (8 years) of PR observations in a study on Hawaii. In our study area, the TRMM product clearly underestimates precipitation by 17–61% (RMSE = 1044 mm) when compared to the measured mean annual precipitation sums. However, the correlation of the pattern with the measured data is high (R^2 = 0.83; Table 2). It can therefore be concluded that although the amounts are not valid without further calibration using regional measurements, the spatial pattern is a valid covariate for precipitation interpolation. For further analysis, the two most promising covariates (*X*-coordinate and TRMM pattern) were chosen to be used for interpolation.

2.3.3. Regression-based interpolation methods

Two regression-based methods, a statistical and a geostatistical method, were tested using the two covariates, one at a time (Table 1). For both methods, a regression equation for the covariate was used to estimate rainfall amounts. This regression equation between rainfall and the covariate was calculated for every wet day using the mean precipitation value of a period of 3 days before and after the interpolation day. A wet day was defined when at least one gauge recorded precipitation on this day. The significance of the regression was tested for every day at the 10% significance level. In case of the *X*-coordinate, we additionally tested if the correlation was negative, because only negative correlation expressed a decline of rainfall from west to east. If these criteria were met (Fig. 4), the regression was used to estimate the mean precipitation for every grid point. In addition, daily residuals for every rain gauge

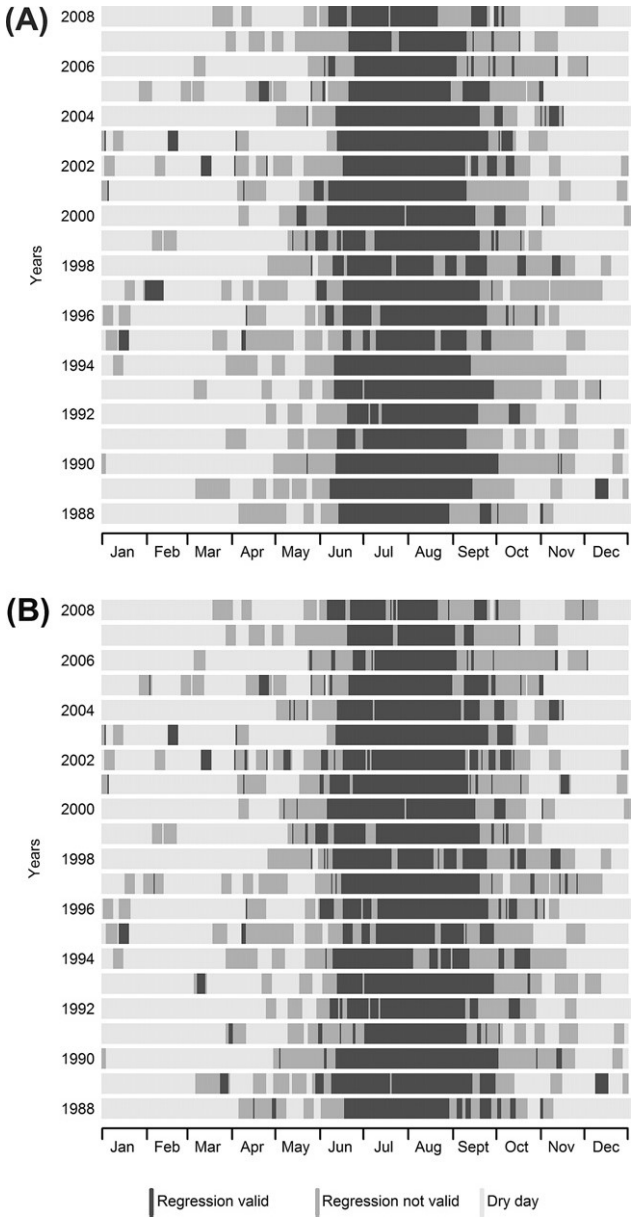

Fig. 4. Validity of the regression approach for (A) covariate *X*-coordinate ($p < 0.1$ and correlation coefficient r<0) and (B) covariate TRMM pattern ($p < 0.1$) for every day from 1988 to 2008.

were calculated by subtracting the regression rainfall from the measured rainfall. It is worth noting that the TRMM pattern can be used more frequently (4% more days) than the *X*-coordinate, if the described criteria are applied. Typically the criteria were met within the rainy season, whereas in the dry season, the local convective rainfall events led to a non-significant relationship with the covariates (Fig. 4). If the criteria were not met, a local IDW approach using the gauges within a 30 km distance was applied. In case of a valid regression, values at every grid point were calculated by adding the explained variance, which is given by the regression, to the unexplained variance, which is expressed by the interpolated residuals. Negative estimates were set to 0 mm rainfall. Either an IDW or a kriging scheme was used to interpolate the residuals. The IDW method can be referred to as regression–inverse distance weighting approach (RIDW) and has previously been applied using elevation as a covariate (e.g., Mauser and Bach, 2009). A local IDW approach using the gauges within a 30 km distance and an optimized exponent of one was used to interpolate the residuals.

As an alternative to the IDW interpolation scheme, a pooled ordinary kriging approach was applied to the residuals. A mean monthly residual was calculated from the daily residuals for every month in every year. These values were pooled to derive residual variograms for every month. A Matern semivariogram model was fitted to these empirical variograms. On the basis of the fitted semivariogram, a local (30 km distance) ordinary kriging approach was applied. Valid variograms were only derived for the rainy season, so that IDW (30 km distance, exponent = 1) was used for interpolation in dry season. Finally, by adding the interpolated residuals to the mean daily rainfall values, calculated from the regression equation, a rainfall estimate was derived for every grid point.

This linear regression–kriging (subsequently referred to as RK) results in the same predictions given the same input parameters as kriging with external drift (Hengl et al., 2007). Both methods allow for incorporation of an external variable that is linearly correlated to the predicted variable (Webster and Oliver, 2007). RK separates regression calculation and residual interpolation and is therefore more flexible, allowing in this case, the combination of day specific regression equations with kriging based on a monthly pooled residual semivariogram.

2.4. Hydrologic model

In this study, the Soil and Water Assessment Tool (SWAT; Arnold et al., 1998) was used to assess the impact of different rainfall interpolation methods on runoff. The SWAT model has proven its capability to model water fluxes also in regions with limited data availability (Ndomba et al., 2008; Stehr et al., 2008). In a preceding study, it was adapted to the Mula–Mutha catchment (Wagner et al., 2011). Thus in the following, we will only present a brief summary of data inputs and model parameterization.

A digital elevation model (DEM) with a spatial resolution of 30 m was derived from ASTER satellite data. This DEM was corrected using a regression with elevation data from topographic maps. The spatial distribution of soils was taken from the digital Soil Map of the World (FAO, 2003). Soil parameterization was partly adapted from a modeling study of the region by Immerzeel et al. (2008), and partly taken from the FAO (2003) database. The land use map was derived from a satellite image taken by LISS-III on the Indian satellite IRS-P6 (Wagner et al., 2011). Crop rotations as well as irrigation schemes were set up for arable land (rice 4.7%, sugarcane 0.7%, mixed cropland 5.3% of the catchment area) to account for the two main cropping seasons in the region. Additionally, the forest growth module was modified to represent the local conditions. For the six major dams in the catchment, a management scheme was developed, which is based on general management rules allowing for water storage in the rainy season and water release in the dry season (Wagner et al., 2011). At the Mulshi and Khadakwasla dams, water is abstracted for energy, irrigation, and water supply purposes. This is incorporated into the model based on a monthly abstraction rate, which is estimated using downstream river gauge measurements. If dams are filled up to 95% of the storage capacity, the abstraction rate is increased to allow for an efficient use of the available water.

Temperature, humidity, solar radiation, and wind speed data were only available at the IMD weather station in Pune (ID 430630, 18.53°N, 73.85°E, 559 m.a.s.l.). Missing temperature values (n = 9 days) were filled using the value of similar days in terms of rain, minimum or maximum temperature, and solar radiation in the same month. Missing humidity (n = 6) and missing wind speed values (n = 10) were filled linearly, by averaging the values of the previous and the following day. On 1269 days, solar radiation values were missing. However, for most of these days some hourly values were available. These were used to fill the hourly data gaps with the hourly observations from a day in the same month with a similar course of solar radiation. The majority of daily missing values (n = 1101) were filled with the help of this procedure. The remaining 168 missing values were filled using the value of a similar day in terms of rain, temperature, and humidity in the same month.

To account for temperature differences within the catchment, temperature values were adjusted for every sub-basin using adiabatic temperature gradients (0.98 °C/100 m on a dry day, 0.44 °C/100 m on a wet day; Weischet, 1995). The two humidity measurements per day in Pune (8:30 am and 5:30 pm) were linearly interpolated to obtain an hourly course of humidity. Mean daily humidity was derived from this hourly course. Relative humidity was calculated for every sub-basin using the sub-basin specific temperature values and the daily specific humidity values measured in Pune. Solar radiation and wind speed from Pune are used for the whole catchment.

Daily discharge data for model validation was only available during rainy seasons between 2001 and 2007. The runoff measurements were quality checked. Values were removed, if the runoff record showed exactly the same value for 3 days in a row. Furthermore, a questionable peak runoff value was found for gauge G1 on 29 and 30 July 2006. For both days, about the same extreme runoff was recorded. This runoff value could not be explained by the measured precipitation. Eliminating the runoff record on 30 July and shifting the runoff measurements 1 day backward between 31 July and 19 September led to a removal of the observed systematic lag between modeled and measured runoff peaks.

The catchment model bases its calculations on 25 sub-basins, which are subdivided into 882 hydrological response units (HRUs). It was run for 21 years from 1988 to 2008, but only 20 years were used for analysis allowing for a 1 year model spin-up phase. To not implicitly correct errors in precipitation measurements with model parameters that were derived from a specific model calibration procedure, we chose default model parameters or we selected the parameters based upon the literature for the given site conditions (e.g. soil parameterization). The values and sources of the parameters that are usually used for calibration in SWAT are provided in the appendix (Table A1). This parameterization procedure has been successfully applied in other studies, where SWAT input parameters were estimated without calibration from readily available GIS databases (e.g., Fontaine et al., 2002; Srinivasan et al., 2010; Zhang et al., 2008). Under similar (Indian) conditions, SWAT showed generally good performances without much calibration (Gosain et al. (2005) only adjusted the low flow (groundwater) component of river runoff). A preceding model application using the same methodology but a different rainfall input was already relatively successful in the study area (Nash-Sutcliffe efficiencies of

0.68 (G1) and 0.58 (G4) at the river gauges that are less affected by dam management; Wagner et al., 2011). Hence, the model was not calibrated with measured runoff data since the focus is set on obvious differences between measured and modeled hydrographs resulting from different rainfall inputs. Four model runs were performed using the different precipitation inputs derived from the regression-based interpolation methods with the *X*-coordinate ($RIDW_X$, RK_X) and the TRMM pattern ($RIDW_{TRMM}$, RK_{TRMM}) as covariate.

2.5. Validation

The interpolation schemes were validated in two steps:

(i) A cross-validation was carried out by estimating the daily time series for the entire period from 1988 to 2008 at one gauge by using all other rain gauges. To evaluate the goodness-of-fit, we calculated root mean square error (RMSE), Nash–Sutcliffe efficiency (NSE; Nash and Sutcliffe, 1970), and percentage bias (PBIAS; Moriasi et al., 2007). The NSE is defined as

$$\mathrm{NSE} = 1 - \frac{\sum_{i=1}^{n}(O_i - M_i)^2}{\sum_{i=1}^{n}(O_i - \overline{O})^2}, \tag{5}$$

and PBIAS is computed in the following way:

$$\mathrm{PBIAS} = 100 \cdot \frac{\sum_{i=1}^{n}(O_i - M_i)}{\sum_{i=1}^{n} O_i}, \tag{6}$$

where O_i is the ith observation, M_i is the ith predicted value, $\overline{O}$ is the mean of the observed values, and n is the total number of observations.

Performances of the different interpolation schemes were ranked for each gauge and hence a mean ranking of each approach was derived by averaging the ranking for all individual gauges. Thus, the best interpolation methods were identified.

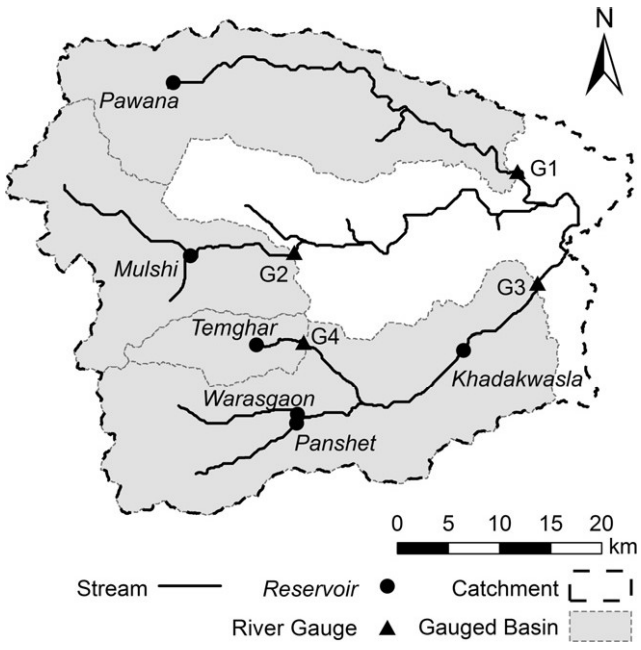

Fig. 5. Location of river gauges and reservoirs in the Mula–Mutha catchment.

(ii) For many environmental applications (such as hydrologic modeling studies) closing the mass balance is of critical importance and reproducing meaningful spatial patterns of rainfall is more important than reproducing point measurements accurately. Therefore, the best approaches identified by cross-validation were compared at the sub-catchment level to assess spatially integrated differences in rainfall and runoff. SWAT was used to evaluate the effects of the different interpolation inputs on the water balance and on runoff dynamics. This validation technique allows for an assessment of the spatially integrated effects of rainfall. It is focused on the two sub-catchments (G1 and G4; Fig. 5) that are less affected by dam management.

3. Results

In general, the interpolation schemes that used covariates outperformed the univariate methods. This is indicated by RMSE, NSE, and PBIAS for the different interpolation schemes and the rankings based on cross-validation using these goodness-of-fit indicators (Table 3). Among the regression-based methods, regression–kriging (RK) and regression–inverse distance weighting (RIDW) showed a similar performance. Comparing the covariates, the use of the *X*-coordinate led to slightly better results than the use of the TRMM pattern as a covariate.

This ranking is also reflected by the performance at the individual gauges as indicated by the NSE (Fig. 6). Except for one station, Thiessen polygons (TH) show the weakest performance, including negative values for three stations. Thiessen polygons typically show reasonable performance for gauges, where the nearby gauge is representative for the estimated gauge (e.g., Kumbheri and Mulshi). If this is not the case, Thiessen polygons do not perform as well as the other methods (e.g., Paud). Ordinary pooled kriging (OK) and IDW perform quite similar with varying performances from gauge to gauge, but significantly better than the Thiessen polygons and slightly worse than the schemes that use covariates. These four regression-based methods often perform similarly. The mean RMSE (Table 3) usually reflects the ranking at the gauges. However, performance varies from one gauge to another. The worst interpolation performance was found at the most eastern gauge Wagholi. As TH and OK show a negative NSE here, it can be concluded that the nearest gauges are not representative for this gauge. The regression-based approaches perform better at this site as they do not rely as much on neighboring gauges, but use information from the covariate. Depending on the chosen goodness-of-fit indicator, the performance of IDW (RMSE; Table 3) and OK (PBIAS; Table 3) is sometimes slightly better than the least best regression-based interpolation method. However taking all indicators into consideration, the regression-based methods show a better performance than the univariate approaches. RK and RIDW can be rated similarly good, as it depends on the rain gauge (Fig. 6) and on the chosen indicator (Table 3) as to which regression-based interpolation method performs best.

For further analysis, the focus is set on the regression-based methods using the two different covariates. Based upon the cross-validation, the incorporation of the *X*-coordinate led to the best interpolation results (Table 3). However, the TRMM data provide spatial patterns that reflect the mean annual distribution of precipitation and incorporate more spatial detail (e.g., orographic rainfall at mountain ridges) than the *X*-coordinate that expresses the general decrease of rainfall with distance from the Western Ghats escarpment.

Despite the small differences of the cross-validation results obtained with the two covariates shown in Table 3, the integrative effect of the chosen covariate is quite obvious at the catchment scale (Table 4), when comparing modeled and measured runoff for two

Table 3
Cross-validation performance and ranking of different interpolation schemes based on root mean square error (RMSE), Nash–Sutcliffe efficiency (NSE), and percentage bias (PBIAS).

Interpolation scheme	Range RMSE (mm)	Mean RMSE (mm)	Rank of mean RMSE	Range NSE	Median NSE	Mean rank of NSE	Rank of mean rank of NSE	Range absolute PBIAS (%)	Mean absolute PBIAS (%)	Rank of mean absolute PBIAS
Thiessen polygons	6.7–20.1	12.3	7	−0.49–0.68	0.26	6.9	7	15.4–41.9	28.0	7
IDW	5.5–19.2	10.1	4	−0.16–0.73	0.57	4.1	5	5.1–53.7	24.0	6
OK	5.6–19.4	10.2	6	−0.17–0.71	0.56	4.3	6	5.6–41.6	19.3	4
$RIDW_X$	5.4–18.1	9.7	1	0.02–0.75	0.60	1.7	1	1.5–41.6	14.8	2
$RIDW_{TRMM}$	5.6–18.3	10.0	3	−0.04–0.73	0.58	3.0	3	2.0–69.1	19.8	5
RK_X	5.4–18.1	9.8	2	0.01–0.75	0.60	1.9	2	2.0–42.7	14.7	1
RK_{TRMM}	5.6–18.4	10.1	5	−0.04–0.72	0.58	3.6	4	1.3–60.0	18.0	3

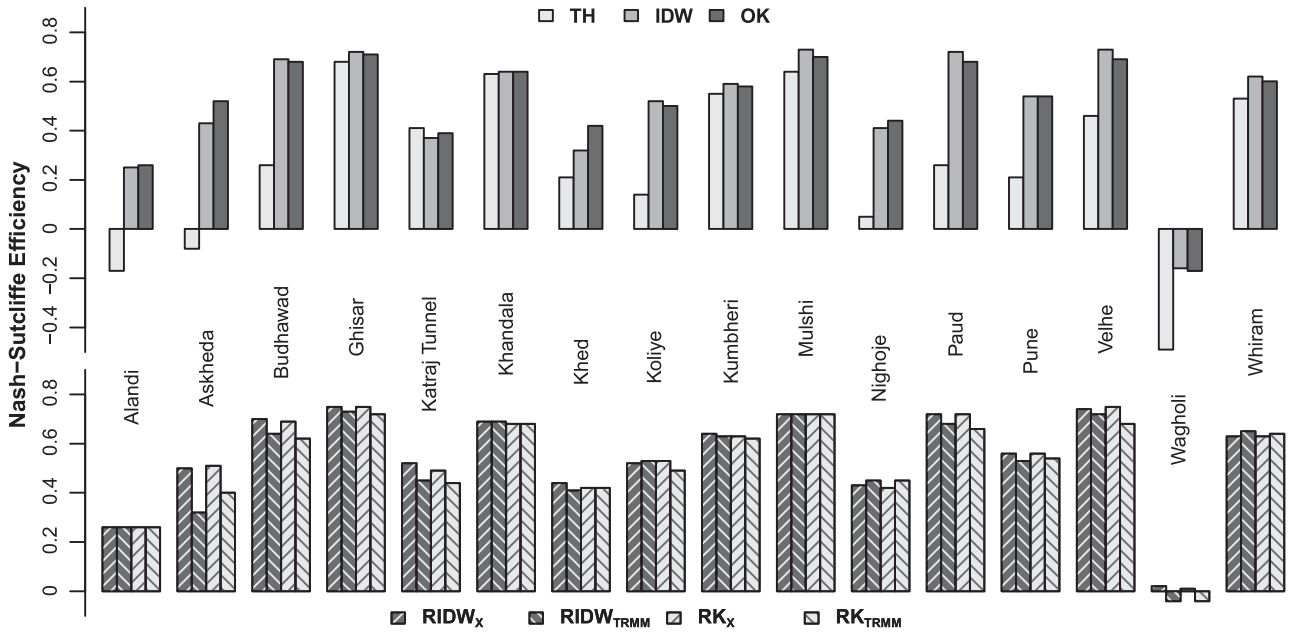

Fig. 6. Interpolation performance at the rain gauges as indicated by the Nash–Sutcliffe efficiency (NSE): Univariate methods above and regression-based methods below.

Table 4
Model performance as indicated by Nash–Sutcliffe efficiency (NSE) and percentage bias (PBIAS) in two sub-catchments using differently interpolated rainfall inputs.

Catchment	G1		G4	
Interpolation scheme	NSE	PBIAS	NSE	PBIAS
$RIDW_X$	0.59	−29.5	0.61	42.9
$RIDW_{TRMM}$	0.73	7.6	0.65	25.6
RK_X	0.61	−28.5	0.62	40.4
RK_{TRMM}	0.68	4.0	0.67	24.4

different sub-catchments (G1 and G4). The performance of the interpolation methods was evaluated using the available daily discharge data during rainy seasons between 2001 and 2007 (Wagner et al., 2011). This evaluation was restricted to sub-catchments G1 and G4, since the measured runoff at gauge G2 and G3 strongly depends upon the management of the upstream dams. Highest NSE and lowest PBIAS values were found when using TRMM data as covariate (Table 4), because TRMM based interpolation led to less precipitation in catchment G1 and to more precipitation in G4 compared to the results using the *X*-coordinate (Table 5). The more favorable NSE and PBIAS indicate that interpolation methods using remotely sensed patterns provide better results with respect to modeled runoff.

The TRMM based methods produce 8.8% and 9.0% (RIDW: 196 mm, RK: 199 mm) higher mean annual precipitation at the catchment scale when compared to the results obtained by using the *X*-coordinate. For the Mula–Mutha catchment the higher

Table 5
Modeled water balance components for the Mula–Mutha catchment and two sub-catchments based on different interpolation schemes.

Sub-catchment	Interpolation scheme	Precipitation (mm)	Runoff (mm)	Evapotranspiration (mm)
Mula–Mutha	$RIDW_X$	2215	1421	731
	$RIDW_{TRMM}$	2410	1573	734
	RK_X	2221	1427	731
	RK_{TRMM}	2420	1585	734
G1	$RIDW_X$	2312	1631	776
	$RIDW_{TRMM}$	1934	1261	767
	RK_X	2308	1625	776
	RK_{TRMM}	1972	1297	766
G4	$RIDW_X$	2630	1972	629
	$RIDW_{TRMM}$	3046	2386	635
	RK_X	2680	2021	630
	RK_{TRMM}	3065	2405	635

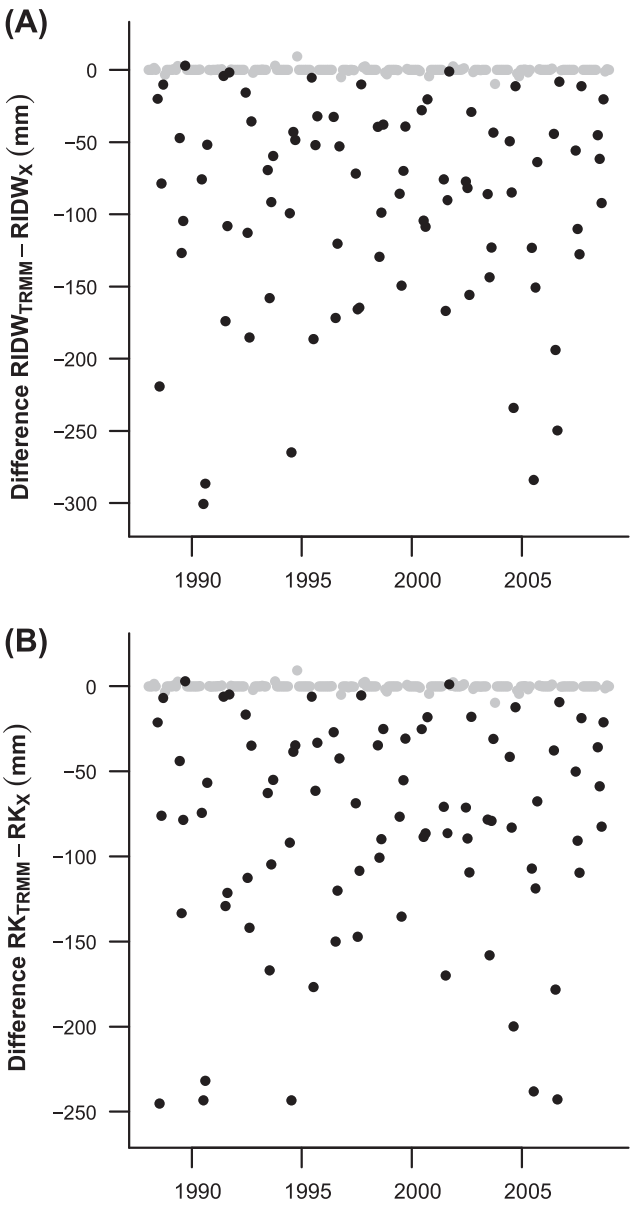

Fig. 7. Differences in monthly rainfall for sub-catchment G1 using different covariates for interpolation: (A) Regression-inverse distance weighting (RIDW) and (B) regression–kriging (RK). Rainy and dry season are shown as black and gray dots, respectively.

rainfall amounts lead to 10.7% and 11.1% (RIDW: 152 mm, RK: 158 mm) higher runoff and only slightly higher evapotranspiration. As has to be expected, the effects of using different covariates are even more pronounced at the sub-catchment scale (Table 5).

In the following paragraphs a more detailed analysis with focus on shorter time scales is presented for sub-catchment G1. Differences between the interpolation methods are more pronounced at shorter time scales. Monthly rainfall differences between RIDW$_{TRMM}$ and RIDW$_X$ in G1 range from −301 mm to +3 mm and from −245 mm to +3 mm for the RK methods (Fig. 7). These monthly differences in sub-catchment G1 generally showed maximum values (>150 mm) in July and August. The resulting differences in runoff dynamics are exemplarily analyzed for monsoon season 2006. This season was chosen since the summed monthly differences for July and August 2006 (RIDW: 444 mm, RK: 421 mm) are largest within the validation period. The course of the hydrograph of the RIDW and RK methods for the same covariate is nearly identical during this period (*X*-coordinate: 0.999 NSE, 0.03% PBIAS; TRMM pattern: 0.987 NSE, −1.09% PBIAS). Thus, the visual analysis shown in Fig. 8 is restricted to comparing the two RK methods. Generally, the higher rainfall amounts of RK$_X$ lead to higher runoff peaks in the respective hydrographs (e.g., 12 and 23 July; Fig. 8). The peaks mostly occur at the same time for both model runs, but may also differ by 1 day (e.g., 15/16 August; Fig. 8). The primarily small differences in June and July add up, so that full storage capacity of the upstream dam is reached at different dates. Hence, once the full storage capacity of the dam is reached, the dampening effect of the dam with respect to runoff peaks ceases to exist. If the full storage capacity is reached at different dates in the models, pronounced differences in runoff may follow (e.g., higher runoff amounts from 30 July to 2 August; Fig. 8). This indicates that different interpolation schemes can make an important difference for runoff dynamics.

Comparing the modeled hydrographs to the measured runoff showed more favorable results using the RK$_{TRMM}$ interpolation (Fig. 8). Particularly during the high flow period between mid July and mid August, the course of the measured runoff is well reproduced by the RK$_{TRMM}$ model. In the early monsoon season before full storage capacity of the dam is reached, both model runs show peaks on 30 June and 6 July that are not represented in the observations. On these dates, the western rain gauges show high amounts of rainfall whereas the eastern gauges show little amounts. Possibly the western gauges were given too much influence in the interpolation on these days. On the other hand, the dampening effect of the dam might be too low in the model. Once the dam is filled, the dampening effect of the dam with respect to the hydrograph is negligible. Hence, the following period is most reliable for comparison of modeled and measured runoff. The poor match in the late monsoon period after mid August may result from dam management impacts that were not represented by the assumed dam management in the model. In contrast to RK$_{TRMM}$, the RK$_X$ interpolation fails to match the dates of the measured peaks in runoff (e.g., peaks on 6, 10, and 16 August; Fig. 8). The modeled peaks occur either 1 day too early or 1 day too late compared to the measured runoff. Furthermore, the integral between measured and modeled hydrograph shows a large overestimation of runoff by the RK$_X$ driven model. This result is underlined by PBIAS, which indicates an overestimation of 28.5% for the whole validation period for RK$_X$. Similarly PBIAS for RK$_{TRMM}$ shows only a small underestimation of 4.0%, which matches well with the generally small integral between measured and RK$_{TRMM}$ modeled runoff in monsoon season 2006. The comparison of runoff dynamics supports the finding that the TRMM pattern is the more suitable covariate to reproduce runoff dynamics.

4. Discussion

The improvement of the interpolation results by using additional information from a covariate (Verworn and Haberlandt, 2011) is very clear in this study, as the regression-based methods outperformed the univariate methods (Table 3 and Fig. 6). This is in agreement with other findings, where external drift kriging (being a modified form of regression kriging) was found to be one of the best interpolation schemes (Goovaerts, 2000; Zhang and Srinivasan, 2009). Pooled semivariograms for rainfall interpolation were previously used only on an event basis (Fiener and Auerswald, 2009; Schuurmans et al., 2007). Our results show that this method can successfully be transferred to monthly pooling, which makes kriging applicable in situations of scarce data availability. However, the superiority of geostatistical methods was not as obvious as in other studies (Buytaert et al., 2006; Goovaerts,

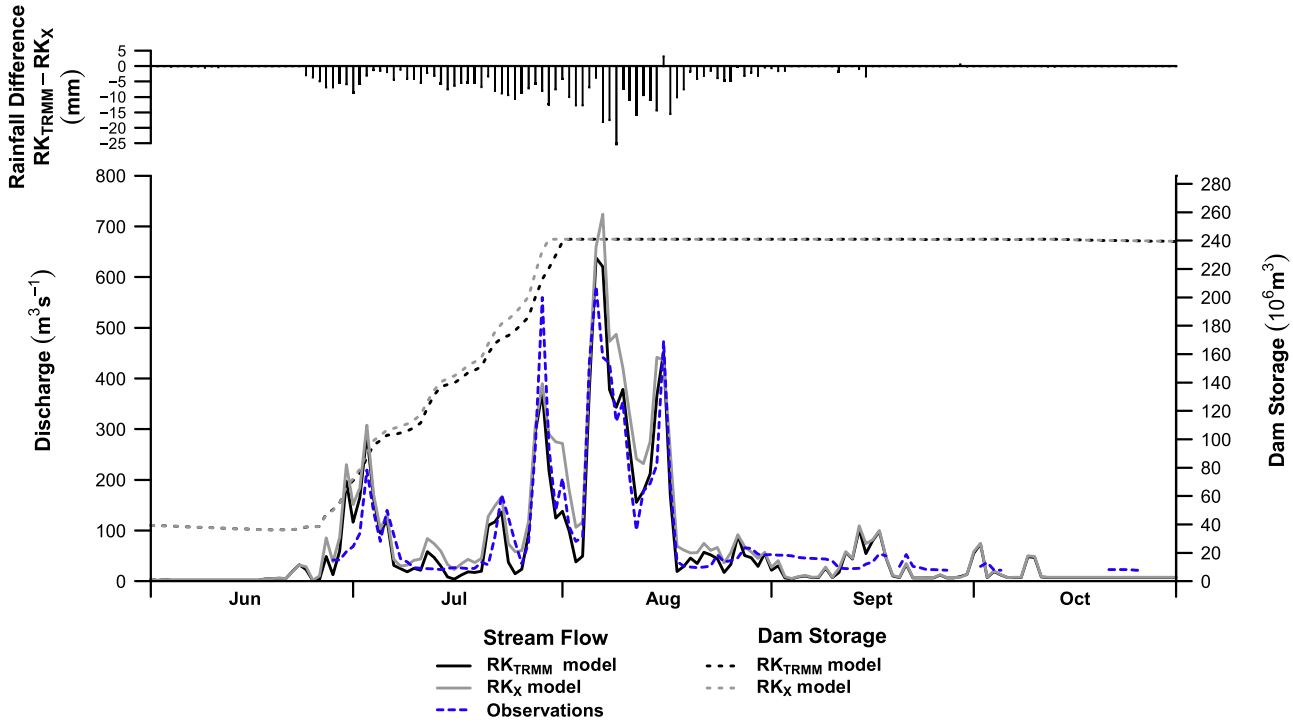

Fig. 8. Modeled and measured runoff at gauge G1, the storage volume of the upstream Pawana dam, and rainfall differences in sub-catchment G1 for regression–kriging rainfall interpolation with covariates TRMM pattern and *X*-coordinate during the 2006 rainy season.

2000; Ly et al., 2011). Two reasons may contribute to this result: (i) In case of the univariate methods the autocorrelation decreases almost linearly with increasing distance (Fig. 2). Thus IDW with an exponent of one is very similar to the applied OK approach. (ii) In case of the regression-based methods the main part of the rainfall estimate is determined by the covariate, giving less influence to the interpolation of the residuals. A major advantage of the IDW method is that it can be used at any time step. Whereas kriging requires a sufficient amount of data to produce a reliable semivariogram, which in our case was achieved by using pooled variograms for every month.

DEM parameters such as elevation are commonly used for rainfall interpolation (Buytaert et al., 2006; Goovaerts, 2000; Lloyd, 2005; Verworn and Haberlandt, 2011). However, a relation between rainfall and elevation could not be found here. If high elevation rainfall measurements are missing or large scale processes dominate the small scale orographic rainfall effects, a relation may not be derived from the data. This is often the case, especially in data scarce regions. In this study, one reason for a missing relation between rainfall and elevation is that the elevation difference of the highest (Katraj Tunnel, 895 m) and the lowest gauge (Pune, 559 m) is not proportionally reflected in the rainfall difference of these gauges. Thus, the mean annual rainfall difference (187 mm) represented by these gauges is small in comparison to the differences in mean annual rainfall, which range up to 3160 mm in the study area. The dominating effect on rainfall distribution is not elevation but distance in wind direction from the Western Ghats escarpment (Table 2), which is expressed by the *X*-coordinate. As the escarpment is the main orographic barrier, the study area lies in the rain shadow of the escarpment. Hence, the potential amount of rainfall at higher mountain ranges to the east of the escarpment (Fig. 1) is limited by the amount of rain that occurred at the escarpment and other westward barriers. The combination of the dominating south-west monsoon and the north–south exposition of the Western Ghats escarpment clearly leads to the west to east decline of rainfall and consequently no rainfall dependence on elevation can be detected in the study area.

An alternative to DEM parameters are satellite measurements of rainfall patterns. For this reason satellite data is increasingly used for rainfall interpolation (Velasco-Forero et al., 2009; Verworn and Haberlandt, 2011; Schiemann et al., 2011). The results show that the annual rainfall pattern that was derived from TRMM precipitation radar is a useful covariate. Within the geographic range of 38°S to 38°N TRMM provides a spatial precipitation pattern, which is an alternative to empirical covariates. Its spatial detail (0.05° grid) makes it superior to empirical covariates such as the *X*-coordinate, which might show a higher correlation with the data, but fail to provide a spatially accurate estimate. Compared to the *X*-coordinate, the TRMM pattern shows a larger spatial variability, which results in some areas in more and in other areas in less rainfall. However, the TRMM based methods provide in any case a better closure of the water balance, as the spatially integrated comparison with measured data shows.

Cross-validation is a widely used and useful technique for the evaluation of interpolation results (Hattermann et al., 2005; Lloyd, 2005). However, with a limited number of values, results are subject to bias that originates from the distribution of the gauges. If this distribution is not representative of the spatial distribution of rainfall, bias is introduced (Heistermann and Kneis, 2011). Particularly in low density measurement networks, interpolation may lead to a large bias, unless these networks were designed with regard to interpolation needs (Cheng et al., 2008). In our study, cross-validation indicated only small differences between RK_{TRMM} and RK_X (RMSE of 10.1 mm and 9.8 mm, Table 3), whereas the spatially integrated assessment showed pronounced differences in the catchment's mean annual rainfall (2420 mm and 2221 mm, Table 5), in monthly rainfall on the sub-catchment scale (Fig. 7), and in runoff dynamics (Fig. 8). While the cross-validation result indicated that RK_X and $RIDW_X$ are the best interpolation technique, the spatially integrated assessment using the SWAT model showed

that RK_{TRMM} and $RIDW_{TRMM}$ are the better interpolation schemes. One reason for this might be the relatively small number of 16 rain gauges. Cross-validation indicated that the interpolation schemes perform similarly at the rain gauge locations. The differences that are exposed by comparing the model based spatially integrated results are due to the different spatial detail provided by the two covariates. The TRMM pattern with its 0.05° resolution was able to reproduce local rainfall effects (e.g., due to topography) better as compared to using the *X*-coordinate as covariate. It can be assumed that a denser rain gauge network (covering also mountain ridges) that better reflects local rainfall effects would probably lead to a decrease of the cross-validation performance of RK_X and $RIDW_X$. In data scarce regions with a high spatial variability in rainfall (such as mountainous areas), cross-validation results should be interpreted with care and should be backed up with a spatially integrated assessment of interpolation quality.

The spatially integrative effect of different interpolation methods can be assessed with hydrologic models, as they spatially integrate precipitation to produce runoff. Hydrographs allow for an evaluation of the interpolated rainfall integrating space and time. However, the approach critically relies on the quality of the model, which needs to accurately represent the catchment's hydrologic response (Heistermann and Kneis, 2011), and on the quality of the measured runoff data. The model should not require much calibration, as calibration might compensate for possibly wrong rainfall input (Heistermann and Kneis, 2011; Strauch et al., 2012). The SWAT model parameters were selected based upon literature values (e.g., soil parameters after Immerzeel et al., 2008), or regional knowledge (e.g., definition of dam management, forest phenology). Otherwise default values were used. The model was not calibrated to observed rainfall–runoff events. Thus, we are confident that the obtained results are not compromised by compensatory effects arising from model calibration. Particularly in consolidated rock catchments such as the Mula–Mutha catchment with its fast system response to precipitation inputs, differences in model response can thus be attributed to the spatial patterns and accuracy of the applied interpolation schemes.

The application of this approach has so far been limited to modeling studies (e.g., Cole and Moore, 2008; Gourley and Vieux, 2005; Heistermann and Kneis, 2011; Hwang et al., 2012). However, the presented results show that it is a suitable method to evaluate interpolation performance. Model based spatial assessment of interpolation accuracy enhances commonly used validation methods and provides reliable results that are particularly valuable in data-scarce regions.

5. Conclusions

In this study, seven interpolation schemes were carried out to provide rainfall data on a daily time step using 16 rain gauges. The different methods were evaluated using a two step validation approach incorporating cross-validation as well as spatially integrated assessment of interpolation performance with the help of a hydrologic model.

Our analysis indicates that precipitation interpolation approaches using appropriate covariates perform best. The two regression-based methods (RIDW and RK) performed similarly well. Since RIDW is less complex than RK, it might be favorable if a quick and straight forward interpolation method is required. Even though its use for interpolation might become more evident in other studies, the additional information that is provided by semivariograms is valuable for analyzing the spatial distribution of rainfall. Monthly pooling is a feasible method to assess autocorrelation of rainfall in data-scarce regions and hence can be used for geostatistical interpolation schemes.

Best interpolation results were obtained using (i) the *X*-coordinate that represents the distance from the Western Ghats escarpment as climatic dominant structure and (ii) the spatial pattern of annual rainfall derived from remotely sensed TRMM precipitation radar. Although the differences in interpolation performance judged by cross-validation were small, relatively large differences in catchment rainfall were recognized for the two best performing interpolation schemes. These differences were even more pronounced focusing on a smaller spatial (sub-catchment) and a smaller time (monthly) scale. A spatially integrated analysis based on rainfall–runoff modeling and its comparison with measured discharge helped to identify the TRMM pattern as a more suitable covariate. Regardless of the sub-catchment, modeled runoff based on the interpolation methods that used the TRMM pattern matched the measured runoff best, because TRMM based interpolation produced more rainfall in one sub-catchment and less rainfall in the other sub-catchment when compared to the interpolation methods that used the *X*-coordinate. The comparatively high spatial resolution of the TRMM pattern provides an accurate estimate of the spatial rainfall distribution, which is particularly important, when interpolated rainfall is used for spatially distributed analysis, such as spatially distributed modeling. Superior to most empirical covariates, the TRMM pattern allows for a transfer of the methodology to other study areas within the geographic range of 38°S to 38°N covered by TRMM. Moreover, it is a valuable alternative to the commonly used covariate elevation, especially in regions where a rainfall dependence on elevation is not present or cannot be derived from measurements.

Furthermore, the results indicate that cross-validation is not sufficient to identify the most suitable precipitation interpolation method in data scarce regions, and that spatially integrated evaluation is needed to assess the accuracy of interpolated spatial rainfall distributions. In this context, hydrologic models are useful tools as they allow for evaluations that are based on runoff, which temporally and spatially integrates rainfall.

In general, our results indicate the high potential of pooled kriging in combination with TRMM data as a covariate (RK_{TRMM}) to derive appropriate daily inputs for hydrologic models in data scarce tropical to sub-tropical regions. Moreover, our study underlines the importance of more sophisticated multi-step validation of interpolations schemes, especially if applied in data scarce regions where cross-validation techniques alone may not be sufficient.

Acknowledgements

We gratefully acknowledge support by a grant from the German National Academic Foundation. We would like to thank Chris Kidd for providing the TRMM rainfall pattern, which was processed by the Earth System Science Interdisciplinary Center, University of Maryland and NASA/Goddard Space Flight Center. We are grateful to IMD Pune, Water Resources Department Nashik, Khadakwasla Irrigation Division Pune, Groundwater Department Pune, Department of Agriculture Pune, and NRSC Hyderabad for supplying environmental data, good cooperation and discussions. Moreover, we acknowledge supply of ASTER data by the USGS Land Processes Distributed Active Archive Center. Special thanks go to Karen Schneider for proof reading the manuscript and to the students from the Institute of Environment Education & Research at Bharati Vidyapeeth University Pune for assistance with the field measurements. The authors thank the editor and the two anonymous reviewers for their helpful comments.

Appendix A

See Table A1.

Table A1
Applied SWAT model parameterization of potential calibration parameters.

Parameter name	Description	Value	Source
CN2	Initial SCS runoff curve number for soil moisture condition II	Depends on soil and land use	Estimated by the model (Neitsch et al., 2010)
SOL_AWC	Available water capacity of the soil layer	Depends on the soil, values given in Wagner et al. (2011)	Immerzeel et al. (2008)
SOL_K	Saturated hydraulic conductivity of the soil layer	Depends on the soil, values given in Wagner et al. (2011)	Immerzeel et al. (2008)
CANMX	Maximum canopy storage	0	Default model parameter value
EPCO	Plant uptake compensation factor	1	Default model parameter value
ESCO	Soil evaporation compensation coefficient	0.95	Default model parameter value
CH_N	Manning's roughness coefficient for channel flow	0.014 s $m^{-1/3}$	Default model parameter value
SURLAG	Surface runoff lag coefficient	4	Default model parameter value
GWQMN	Threshold depth of water in the shallow aquifer required for return flow to occur	0 mm	Default model parameter value
GW_DELAY	Groundwater delay time	31 d	Default model parameter value
GW_REVAP	Groundwater "revap" coefficient	0.02	Default model parameter value
ALPHA_BF	Baseflow alpha factor	0.048 d	Default model parameter value
REVAPMN	Threshold depth of water in the shallow aquifer for "revap" or percolation to the deep aquifer to occur	1 mm	Default model parameter value

References

Arnold, J.G., Srinivasan, R., Muttiah, R.S., Williams, J.R., 1998. Large area hydrologic modeling and assessment – Part 1: Model development. J. Am. Water Resour. Assoc. 34, 73–89.

Barros, A.P., Lettenmaier, D.P., 1993. Dynamic modeling of the spatial distribution of precipitation in remote mountainous areas. Mon. Weather Rev. 121, 1195–1214.

Barry, R.G., 1992. Mountain climatology and past and potential future climatic changes in mountain regions. Mt. Res. Dev. 12 (1), 71–86.

Basistha, A., Arya, D.S., Goel, N.K., 2008. Spatial distribution of rainfall in Indian Himalayas—a case study of Uttarakhand Region. Water Resour. Manage 22, 1325–1346.

Beven, K.J., 2001. Rainfall–runoff Modelling: The Primer. John Wiley & Sons Ltd., Chichester.

Burrough, P.A., McDonnell, R.A., 1998. Principles of Geographical Information Systems. Oxford University Press, Oxford.

Buytaert, W., Celleri, R., Willems, P., De Bièvre, B., Wyseure, G., 2006. Spatial and temporal rainfall variability in mountainous areas: a case study from the south Ecuadorian Andes. J. Hydrol. 329, 413–421.

Carrera-Hernández, J.J., Gaskin, S.J., 2007. Spatio temporal analysis of daily precipitation and temperature in the Basin of Mexico. J. Hydrol. 336, 231–249.

Chaubey, I., Haan, C.T., Salisbury, J.M., Grunwald, S., 1999. Quantifying model output uncertainty due to the spatial variability of rainfall. J. Am. Water Resour. Assoc. 35 (5), 1113–1123.

Cheng, K.-S., Lin, Y.-C., Liou, J.-J., 2008. Rain-gauge network evaluation and augmentation using geostatistics. Hydrol. Process. 22, 2554–2564.

Cole, S.J., Moore, R.J., 2008. Hydrological modeling using raingauge- and radar-based estimators of areal rainfall. J. Hydrol. 358, 159–181.

Croke, B.F.W., Islam, A., Ghosh, J., Khan, M.A., 2011. Evaluation of approaches for estimation of rainfall and the unit hydrograph. Hydrol. Res. 42 (5), 372–385.

Di Piazza, A., Lo Conti, F., Noto, L.V., Viola, F., La Loggia, G., 2011. Comparative analysis of different techniques for spatial interpolation of rainfall data to create a serially complete monthly time series of precipitation for Sicily, Italy. Int. J. Appl. Earth Obs. Geoinf. 13, 396–408.

Fiener, P., Auerswald, K., 2009. Spatial variability of rainfall on a sub-kilometre scale. Earth Surf. Process. Landforms 34, 848–859.

Fontaine, T.A., Cruickshank, T.S., Arnold, J.G., Hotchkiss, R.H., 2002. Development of a snowfall–snowmelt routine for mountainous terrain for the soil water assessment tool (SWAT). J. Hydrol. 262, 209–223.

Food and Agriculture Organization of the United Nations (FAO), 2003. Digital Soil Map of the World and Derived Soil Properties, FAO, Rome.

Gadgil, A., 2002. Rainfall characteristics of Maharashtra. In: Diddee, J., Jog, S.R., Kale, V.S., Datye, V.S. (Eds.), Geography of Maharashtra. Rawat Publications, Jaipur, pp. 89–102.

Goovaerts, P., 2000. Geostatistical approaches for incorporating elevation into the spatial interpolation of rainfall. J. Hydrol. 228, 113–129.

Gosain, A.K., Rao, S., Srinivasan, R., Reddy, N.G., 2005. Return-flow assessment for irrigation command in the Palleru river basin using SWAT model. Hydrol. Process. 19, 673–682.

Gourley, J.J., Vieux, B.E., 2005. A method for evaluating the accuracy of quantitative precipitation estimates from a hydrologic modeling perspective. J. Hydrometeorol. 6 (2), 115–133.

Gunnell, Y., 1997. Relief and climate in South Asia: the influence of the Western Ghats on the current climate pattern of peninsular India. Int. J. Climatol. 17, 1169–1182.

Hattermann, F., Krysanova, V., Wechsung, F., Wattenbach, M., 2005. Runoff simulations on the macroscale with the ecohydrological model SWIM in the Elbe catchment – validation and uncertainty analysis. Hydrol. Process. 19, 693–714.

Heistermann, M., Kneis, D., 2011. Benchmarking quantitative precipitation estimation by conceptual rainfall–runoff modeling. Water Resour. Res. 47, W06514.

Hengl, T., Heuvelink, G.B.M., Rossiter, D.G., 2007. About regression–kriging: from equations to case studies. Comput. Geosci. 33, 1301–1315.

Hwang, Y., Clark, M., Rajagopalan, B., Leavesley, G., 2012. Spatial interpolation schemes of daily precipitation for hydrologic modeling. Stoch. Environ. Res. Risk Assess. 26, 295–320.

Immerzeel, W.W., Gaur, A., Zwart, S.J., 2008. Integrating remote sensing and a process-based hydrological model to evaluate water use and productivity in a south Indian catchment. Agric. Water Manage. 95, 11–24.

Jain, S.K., Agarwal, P.K., Singh, V.P., 2007. Hydrology and Water Resources of India. Springer, Dordrecht.

Kidd, C., McGregor, G., 2007. Observation and characterisation of rainfall over Hawaii and surrounding region from the Tropical Rainfall Measuring Mission. Int. J. Climatol. 27 (4), 541–553.

Kummerow, C., Simpson, J., Thiele, O., Barnes, W., Chang, A.T.C., Stocker, E., Adler, R.F., Hou, A., Kaker, R., Wentz, F., Ashcroft, P., Kozu, T., Hong, Y., Okamoto, K., Iguchi, T., Kuroiwa, H., Im, E., Haddad, Z., Huffman, G., Ferrier, B., Olson, W.S., Zipser, E., Smith, E.A., Wilheit, T.T., North, G., Krishnamurti, T., Nakamura, K., 2000. The status of the tropical rainfall measuring mission (TRMM) after two years in orbit. J. Appl. Meteorol. 39, 1965–1982.

Kurtzman, D., Navon, S., Morin, E., 2009. Improving interpolation of daily precipitation for hydrologic modelling: spatial patterns of preferred interpolators. Hydrol. Process. 23, 3281–3291.

Lloyd, C.D., 2005. Assessing the effect of integrating elevation data into the estimation of monthly precipitation in Great Britain. J. Hydrol. 308, 128–150.

Ly, S., Charles, C., Degré, A., 2011. Geostatistical interpolation of daily rainfall at catchment scale: the use of several variogram models in the Ourthe and Ambleve catchments, Belgium. Hydrol. Earth Syst. Sci. 15, 2259–2274.

Mauser, W., Bach, H., 2009. PROMET – large scale distributed hydrological modelling to study the impact of climate change on the water flows of mountain watersheds. J. Hydrol. 376, 362–377.

Moriasi, D.N., Arnold, J.G., Van Liew, M.W., Bingner, R.L., Harmel, R.D., Veith, T.L., 2007. Model evaluation guidelines for systematic quantification of accuracy in watershed simulations. Trans. ASABE 50 (3), 885–900.

Nash, J.E., Sutcliffe, J.V., 1970. River flow forecasting through conceptual models part I – a discussion of principles. J. Hydrol. 10, 282–290.
Ndomba, P., Mtalo, F., Killingtveit, A., 2008. SWAT model application in a data scarce tropical complex catchment in Tanzania. Phys. Chem. Earth 33, 626–632.
Neitsch, S.L., Arnold, J.G., Kiniry, J.R., Srinivasan, R., Williams, J.R., 2010. Soil and Water Assessment Tool: Input/Output File Documentation, Version 2009. Texas Water Resources Institute, Texas A&M University, College Station, Texas.
Pebesma, E.J., 2004. Multivariable geostatistics in S: the gstat package. Comput. Geosci. 30, 683–691.
R Development Core Team, 2011. R: A Language and Environment for Statistical Computing. Ver. 2.13.0. R Foundation for Statistical Computing, Vienna.
Richter, D., 1995. Ergebnisse methodischer Untersuchungen zur Korrektur des systematischen Meßfehlers des Hellmann-Niederschlagmessers. Berichte des Deutschen Wetterdienstes 194, Offenbach.
Schiemann, R., Erdin, R., Willi, M., Frei, C., Berenguer, M., Sempere-Torres, D., 2011. Geostatistical radar-raingauge combination with nonparametric correlograms: methodological considerations and application in Switzerland. Hydrol. Earth Syst. Sci. 15, 1515–1536.
Schuurmans, J.M., Bierkens, M.F.P., Pebesma, E.J., Uijlenhoet, R., 2007. Automatic prediction of high-resolution daily rainfall fields for multiple extents: the potential of operational radar. J. Hydrometeorol. 8 (6), 1204–1224.
Searcy, J.K., Hardison, C.H., Langbein, W.B., 1960. Double mass curves. Geological Survey Water Supply Paper 1541-B. US Geological Survey, Washington DC.
Shepard, D., 1968. A two-dimensional interpolation function for irregularly-spaced data. In: Blue, R.B., Sr., Rosenberg, A.M. (Eds.), Proceedings of the 1968 23rd ACM National Conference. August 27–29. ACM Press, New York, pp. 517–524.
Srinivasan, R., Zhang, X., Arnold, J.G., 2010. SWAT ungauged: hydrological budget and crop yield predictions in the upper Mississippi river basin. Trans. ASABE 53 (5), 1533–1546.
Stehr, A., Debels, P., Romero, F., Alcayaga, H., 2008. Hydrological modelling with SWAT under conditions of limited data availability: evaluation of results from a Chilean case study. Hydrol. Sci. J. 53, 588–601.
Stein, M.L., 1999. Interpolation of Spatial Data: Some Theory for Kriging. Springer, New York.
Strauch, M., Bernhofer, C., Koide, S., Volk, M., Lorz, C., Makeschin, F., 2012. Using precipitation data ensemble for uncertainty analysis in SWAT streamflow simulation. J. Hydrol. 414–415, 413–424.
Tabios, G.Q., Salas, J.D., 1985. A comparative analysis of techniques for spatial interpolation of precipitation. J. Am. Water Resour. Assoc. 21, 365–380.
Teegavarapu, R.S.V., Tufail, M., Ormsbee, L., 2009. Optimal functional forms for estimation of missing precipitation data. J. Hydrol. 374, 106–115.
Thiessen, A.H., 1911. Precipitation averages for large areas. Mon. Weather Rev. 39 (7), 1082–1084.
Velasco-Forero, C.A., Sempere-Torres, D., Cassiraga, E.F., Gómez-Hernández, J.J., 2009. A non-parametric automatic blending methodology to estimate rainfall fields from rain gauge and radar data. Adv. Water Resour. 32, 986–1002.
Verworn, A., Haberlandt, U., 2011. Spatial interpolation of hourly rainfall – effect of additional information, variogram inference and storm properties. Hydrol. Earth Syst. Sci. 15, 569–584.
Voltz, M., Webster, R., 1990. A comparison of kriging, cubic splines and classification for predicting soil properties from sample information. J. Soil Sci. 41, 473–490.
Wackernagel, H., 2003. Multivariate Geostatistics: An Introduction with Applications, third ed. Springer, New York.
Wagner, P.D., Kumar, S., Fiener, P., Schneider, K., 2011. Hydrological modeling with SWAT in a monsoon-driven environment: experience from the Western Ghats. India. Trans. ASABE 54 (5), 1783–1790.
Webster, R., Oliver, M.A., 2007. Geostatistics for Environmental Scientists, second ed. John Wiley & Sons Ltd., Chichester.
Weischet, W., 1995. Einführung in Die Allgemeine Klimatologie, sixth ed. Teubner, Stuttgart.
Winchell, M., Srinivasan, R., Di Luzio, M., Arnold, J., 2010. ArcSWAT Interface for SWAT2009. User's Guide. Blackland Research Center, Texas Agricultural Experiment Station and Grassland, Soil and Water Research Laboratory, USDA Agricultural Research Service, Temple, Texas.
Zhang, X., Srinivasan, R., 2009. GIS-based spatial precipitation estimation: a comparison of geostatistical approaches. J. Am. Water Resour. Assoc. 45 (4), 894–906.
Zhang, X., Srinivasan, R., Debele, B., Hao, F., 2008. Runoff simulation of the headwaters of the Yellow River using the SWAT model with three snowmelt algorithms. J. Am. Water Resour. Assoc. 44 (1), 48–61.